1521-0111/12/8103-393–400$25.00
MOLECULAR PHARMACOLOGY
Vol. 81, No. 3
76281/3749621

Mol Pharmacol 81:393–400, 2012

Covalent Modification of a Volatile Anesthetic Regulatory Site Activates TASK-3 (KCNK9) Tandem-Pore Potassium Channels[S]

Kevin E. Conway and Joseph F. Cotten

Department of Anesthesia, Critical Care, and Pain Medicine, Massachusetts General Hospital, Boston, Massachusetts

Received October 11, 2011; accepted December 6, 2011

ABSTRACT

TASK-3 (KCNK9) tandem-pore potassium channels provide a volatile anesthetic-activated and $G\alpha_q$ protein- and acidic pH-inhibited potassium conductance important in neuronal excitability. Met-159 of TASK-3 is essential for anesthetic activation and may contribute to the TASK-3 anesthetic binding site(s). We hypothesized that covalent occupancy of an anesthetic binding site would irreversibly activate TASK-3. We introduced a cysteine at residue 159 (M159C) and studied the rate and effect of Cys-159 modification by *N*-ethylmaleimide (NEM), a cysteine-selective alkylating agent. TASK-3 channels were transiently expressed in Fischer rat thyroid cells, and their function was studied in an Ussing chamber. NEM irreversibly activated M159C TASK-3, with minimal effects on wild-type TASK-3. NEM-modified M159C channels were resistant to inhibition by both acidic pH and active $G\alpha_q$ protein. M159C channels that were first inhibited by $G\alpha_q$ protein were more-slowly activated by NEM, which suggests protection of Cys-159, and similar results were observed with isoflurane activation of wild-type TASK-3. M159W and M159F TASK-3 mutants behaved like NEM-modified M159C channels, with increased basal currents and resistance to inhibition by active $G\alpha_q$ protein or acidic pH. TASK-3 wild-type/M159C dimers expressed as a single polypeptide demonstrated that modification of a single Cys-159 was sufficient for TASK-3 activation, and M159F/M159C and M159W/M159C dimers provided evidence for cross-talk between subunits. The data are consistent with residue 159 contributing to an anesthetic regulatory site or sites, and they suggest that volatile anesthetics, through perturbations at a single site, increase TASK-3 channel activity and disrupt its regulation by active $G\alpha_q$ protein, a determinant of central nervous system arousal and consciousness.

Introduction

Tandem-pore potassium channels provide background potassium conductance important in the determination of neuronal resting membrane potentials and excitability (Yost, 2003). Volatile anesthetic activation of these channels, which causes neuronal hyperpolarization and quiescence, may underlie some clinical effects such as unconsciousness and immobility during noxious stimuli. The TASK-3 (KCNK9) channel is a member of the tandem-pore family that is widely expressed in the nervous system, and its function is activated by all halogenated volatile anesthetics in current clinical use (Kim et al., 2000). Studies with TASK-3-knockout mice confirmed the relevance of this channel. Compared with wild-type control mice, TASK-3-knockout mice require increased amounts of volatile anesthesia for loss of consciousness and immobility, are slower to lose consciousness, and, in the absence of anesthesia, display fragmented sleep (Pang et al., 2009; Lazarenko et al., 2010).

The molecular mechanisms through which volatile anesthetics activate TASK-3 are poorly understood. Studies of the TASK-3 homolog TASK-1 by Patel et al. (1999) identified the carboxyl terminus, and more specifically amino acids 243 to 248 (VLRFMT) in the proximal carboxyl terminus, as essential for halothane activation. Later work by Talley and Bayliss (2002) determined that the carboxyl terminus was important for halothane activation of TASK-3 as well, and the authors demonstrated that graded deletions of the carboxyl terminus caused graded decreases in halothane activation. Across a range of carboxyl terminus deletion constructs, the authors noted a correlation between loss of halothane activation and loss of $G\alpha_{q/11}$-coupled G protein-coupled receptor (GPCR) inhibition, which suggests commonalities in the mechanisms of action. Their TASK-3/TREK-1 mutant involving proximal carboxyl-terminal residues 243 to 248 (VLRFLT) was resistant to both anesthetic and GPCR regulation (Fig. 1A).

This research was supported by grants from the Foundation for Anesthesia Education and Research and the National Institutes of Health National Institute of General Medical Sciences [Grant GM083216].

Article, publication date, and citation information can be found at http://molpharm.aspetjournals.org.

http://dx.doi.org/10.1124/mol.111.076281.

[S] The online version of this article (available at http://molpharm.aspetjournals.org) contains supplemental material.

ABBREVIATIONS: FRT, Fischer rat thyroid; GPCR, G protein-coupled receptor; NEM, *N*-ethylmaleimide; PIP_2, phosphatidylinositol 4,5-bisphosphate; MES, 4-morpholineethanesulfonic acid.

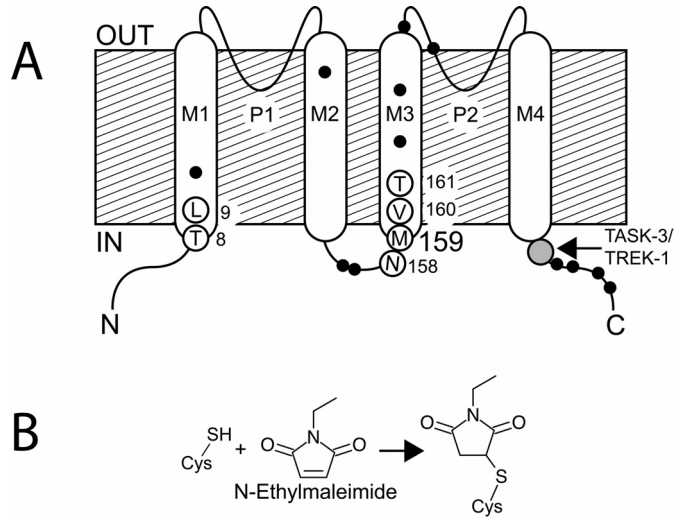

Fig. 1. Schematic diagram of the TASK-3 (KCNK9) potassium channel subunit (A) and NEM modification of the cysteine residue (B). Transmembrane segments M1, M2, M3, and M4 and the two pore-contributing P-loop domains (P1 and P2) are labeled. The membrane is hatched, with intracellular (IN) and extracellular (OUT) surfaces indicated. The locations of residue Met-159 and others residues mutated to cysteine in this study are shown. Black dots, locations of the 12 endogenous cysteine residues (Cys-14, -110, -146, -147, -167, -172, -181, -193, -296, -299, -354, and -383). Large gray dot, site of the TASK-3/TREK-1 mutation in which amino acids 243 to 248 (VLRFLT) were mutated to GDWLRV. B, chemical structure of NEM and its cysteine thioether derivative.

There is also limited understanding of volatile anesthetic binding by TASK-3. Met-159, which was predicted to reside in the intracellular portion of the third transmembrane domain on the basis of hydropathic analysis (Fig. 1A) (Kim et al., 2000), was identified by Andres-Enguix et al. (2007) as a potential volatile anesthetic binding site. Met-159 is essential for halothane, isoflurane, and chloroform activation of both TASK-3 and its two homologs, LyTASK and TASK-1. Loss of (*R*)- and (*S*)-isoflurane stereoselectivity in the L159A LyTASK mutant suggested altered anesthetic binding effects. The role of Met-159 in GPCR regulation of TASK-3 has not been addressed.

Cysteine modification is a powerful tool for studying ion channel structure and function and has proved useful for studying anesthetic interactions with ion channels (Cotten and Welsh, 1998; Lobo et al., 2006). We adopted this technique to study the role of residue 159 in TASK-3 regulation by volatile anesthetics and GPCRs. We hypothesized that, if residue 159 were within a TASK-3 anesthetic binding site, then covalent occupancy of this site would markedly increase TASK-3 channel activity. We also hypothesized that, if residue 159 were involved in GPCR regulation, then NEM modification of Cys-159 might alter this regulation, and, conversely, GPCR effects might modify Cys-159 reactivity. To test these hypotheses, we prepared the M159C TASK-3 mutant, expressed it in Fischer rat thyroid cells, and studied its functional response to *N*-ethylmaleimide (NEM) in the absence and presence of activated m1 muscarinic GPCRs or constitutively active $G\alpha_q$ protein. NEM, which reacts selectively and irreversibly with cysteines (Fig. 1B), minimally affects wild-type TASK-3 and is uncharged, such that it can cross the cell membrane.

Materials and Methods

Molecular Biology Procedures. Rat TASK-3, human m1 muscarinic GPCR, and human $G\alpha_q$ protein cDNAs were used. LyTASK cDNA from *Lymnae stagnalis* was a generous gift from Dr. Nicholas Franks (Imperial College, London, UK). Variants of the pcDNA3.1 vector (Invitrogen, Carlsbad, CA) were used for transient cDNA expression. Mutant human Q209L $G\alpha_q$ protein and human m1 muscarinic receptor cDNA were obtained from the Missouri S&T cDNA Resource Center (Rolla, MO). Mutations were introduced through high-fidelity polymerase chain reactions using QuikChange mutagenesis (Stratagene, Santa Clara, CA) or through overlapping extension and were confirmed through bidirectional sequencing (Massachusetts General Hospital DNA Core Facility, Boston, Massachusetts). The TASK-3 dimers were prepared by ligating a polymerase chain reaction fragment encoding wild-type, M159W, M159F, or M159A TASK-3 cDNA, minus its stop codon, between HindIII and KpnI restriction sites upstream of the M159C-TASK3 coding sequence in the pcDNA3.1/V5-His-TOPO-TA vector (Invitrogen). This introduced an 18-amino acid linker sequence (LVPSSDPLVQCGGIALAT) between TASK-3 subunits. The m1 muscarinic GPCR stable cell line was derived by using a lentivirus; m1 muscarinic cDNA was cloned into CSCW2-IRES-mCherry for lentivirus preparation (Massachusetts General Hospital Vector Core). After infection, the stable cell line was expanded from a single clone identified and isolated on the basis of mCherry fluorescence (Massachusetts General Hospital Flow Cytometry Core).

Expression and Electrophysiological Behavior in Fischer Rat Thyroid Epithelia. Fischer rat thyroid (FRT) epithelial cells (Sheppard et al., 1994) were cultured at 37°C and 5% CO_2 in a humidified incubator, by using Ham's F-12 medium (Sigma-Aldrich, St. Louis, MO) supplemented with 5% fetal calf serum (Sigma-Aldrich). Cells were trypsinized, placed on semipermeable supports ($\sim 1.5 \times 10^5$ cells per support; Snapwell polycarbonate supports, 0.4-μm pore size, 12-mm diameter; Corning Life Sciences, Lowell, MA), and transfected in suspension by using Lipofectamine 2000 (Invitrogen). FRT epithelial monolayers were studied 48 h after transfection in an Ussing chamber (Physiologic Instruments, San Diego, CA). Junction potentials were offset before each experiment. A potassium gradient was applied across the monolayer. Apical solution contained 135 mM NaCl, 1.2 mM $MgCl_2$, 1.2 mM $CaCl_2$, 10 mM HEPES, and 10 mM dextrose (pH adjusted to 7.4 with NaOH), and basolateral solution contained 135 mM KCl, 1.2 mM $MgCl_2$, 1.2 mM $CaCl_2$, 10 mM HEPES, and 10 mM dextrose (pH adjusted to 7.4 with KOH). MES was used instead of HEPES in solutions of pH 6.0 or below. Maleimide reagent stock (1 M in dimethyl sulfoxide) was prepared fresh daily. Maleimides and carbachol were applied simultaneously to both the apical and basal chambers; acidic/alkaline pH solutions were applied to the apical side only. In all studies, the transepithelial voltage was clamped at 0 mV; the potassium concentration gradient provided the driving force for potassium flux (>100 mV, according to the Nernst equation). A DVC-1000 amplifier (World Precision Instruments, Sarasota, FL) amplified the signal, which was digitized with no filtering at 10 Hz by using a USB-6009 data acquisition board (National Instruments, Austin, TX) interfaced with an Apple computer (Apple, Cupertino, CA) running Labview 8.5 software (National Instruments). Data were averaged every 1 s for analysis. Positive current indicates positive charge flowing in the basolateral-to-apical direction. Transepithelial voltage pulses of +5 mV (1-s duration), referenced to the apical surface, were applied intermittently to assess transepithelial resistance and monolayer integrity. Air was bubbled continuously through the apical and basolateral solutions. All studies were conducted at room temperature (22–24°C).

Volatile Anesthetic Application. Isoflurane (Baxter Healthcare, Deerfield, IL) was applied with a Datex Ohmeda variable-bypass vaporizer (GE Healthcare, Chalfont St. Giles, Buckinghamshire, UK) in series with the air flow (2 liters/min) providing mixing bubbles to the Ussing chamber. Gas flow distal to the chamber was

sampled continuously and analyzed in real time for anesthetic concentrations by using a calibrated Datex Capnomac Ultima medical gas analyzer (GE Healthcare). To account for the temperature dependence of isoflurane aqueous solubility, isoflurane gas concentrations (in percentage atmospheres) determined at room temperature with the gas analyzer were converted to solute concentrations (in millimolar) by using the methods described by Franks and Lieb (1993), with the assumption of an Ostwald water/gas room temperature partition coefficient of 1.21.

Graphing and Statistical Analysis. All data are reported as mean ± S.E.M. Data analysis, graphing, and regression were performed by using Microsoft Excel (Microsoft, Redmond, WA), Prism 5.0 (GraphPad Software, La Jolla, CA), and Adobe Illustrator CS4 (Adobe Systems, San Jose, CA) software. Statistical significance ($P < 0.05$) was determined by using, where appropriate, a Student's t test or one-way analysis of variance, followed by a post hoc Newman-Keuls test or Bonferroni test.

For quantification of the rate and magnitude of changes in potassium currents after NEM or isoflurane application, the signal was fit with a one- or two-phase exponential function through nonlinear regression, as follows: one phase, $I = I_{basal} + [[I_{plateau} - I_{basal}] \times [1 - \exp(-t/\tau)]]$; two phase, $I = I_{basal} + [A[I_{plateau} - I_{basal}] \times [1 - \exp(-t/\tau_1)]] + [(1 - A)[I_{plateau} - I_{basal}] \times [1 - \exp(-t/\tau_2)]]$. I_{basal} is the steady-state current just before NEM or isoflurane application, $I_{plateau}$ is the maximal current achieved with NEM or isoflurane, A is a scaling coefficient of ≤1, and t is time. A composite $\tau = A\tau_1 + (1 - A)\tau_2$ was derived to facilitate some comparisons. Rate values ($1/\tau$) are reported in the figures. Percentage changes in current were reported relative to the basal current immediately before isoflurane or NEM application by using the following equation: activation = $(I_{plateau}/I_{basal} - 1) \times 100$. $I_{plateau}$ and I_{basal} were derived from fitted curves or through visual inspection, when data were not fitted.

Reagents. All chemical supplies and reagents were obtained from Sigma-Aldrich or Thermo Fisher Scientific (Waltham, MA) unless noted otherwise.

Results

NEM Activates M159C TASK-3 and Its Homolog L159C LyTASK. FRT monolayers transfected with M159C TASK-3 or wild-type subunits displayed positive transepithelial potassium currents that were inhibited at acidic pH (Fig. 2). NEM irreversibly potentiated potassium currents conducted by M159C TASK-3 but minimally affected those conducted by wild-type TASK-3 (Figs. 2, A and B, and 3). The concentration dependence of the NEM modification rate was linear, and there was a small NEM concentration dependence for potentiation (Fig. 2C). Isoflurane, which may bind at or near residue 159 of the wild-type subunit, had no effect on the NEM rate of modification or the magnitude of potentiation (Fig. 2C). The NEM vehicle alone (dimethyl sulfoxide at 0.1% or 1%) had minimal effects on M159C TASK-3 function, causing slight inhibition (1 ± 1% and 5 ± 1%, respectively; $n = 3$). TASK-3 subunits with cysteine residues introduced at sites adjacent to residue 159 (N158C, V160C, and T161C) or at analogous sites in the first half of TASK-3 (T8C and L9C) (Figs. 1 and 3) were minimally affected by NEM. It is noteworthy that the TASK-3/TREK-1 mutation (Fig. 1A), which renders TASK-3 channels resistant to activation by volatile anesthetics, also decreased NEM activation of M159C TASK-3 channels (Fig. 3; Supplemental Fig. 1). Other maleimide reagents, both smaller and larger (i.e., maleimide and *N*-propylmaleimide, both at 1 mM), activated M159C TASK-3 (maleimide, 190 ± 40%, $\tau = 140 \pm 11$ s, $n = 10$; *N*-propylmaleimide, 258 ± 49%, $\tau = 75 \pm 7$ s, $n = 12$).

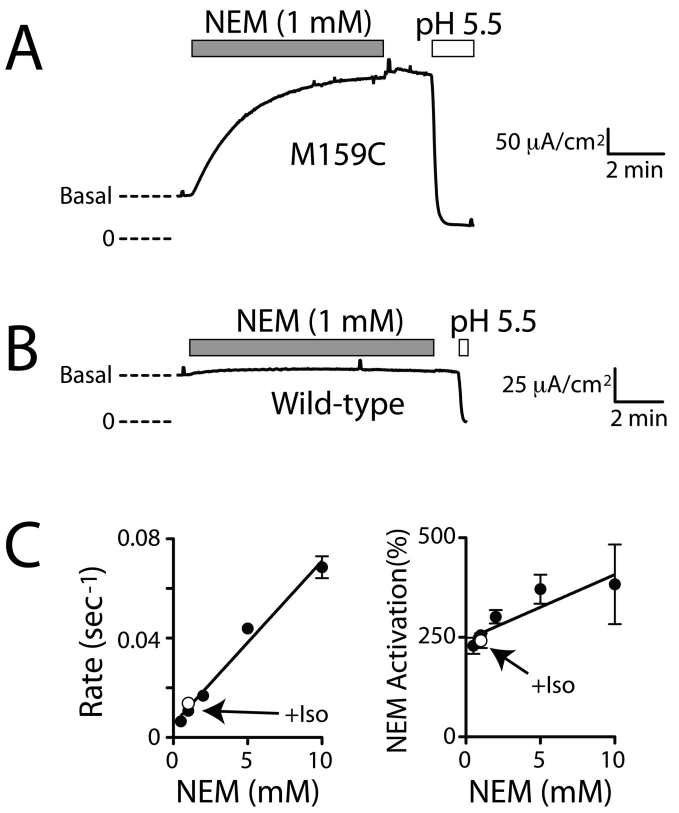

Fig. 2. Irreversible activation by NEM of M159C but not wild-type TASK-3 potassium currents. A and B, Ussing chamber transepithelial current records from FRT monolayers transfected with M159C (A) or wild-type (B) TASK-3 potassium channel subunit cDNA. Gray bars, application of NEM; white bars, apical application of acidic pH. In A and B, the dashed lines indicate the monolayer zero-current levels and the basal potassium current levels (I_{basal}) used for calculation of NEM activation (see *Materials and Methods*). Black bars, current and time scales. C, NEM concentration dependence of M159C modification and activation. Data in C were obtained from a single exponential fit to individual current records, as described in *Materials and Methods* ($n = 4$ each, mean ± S.E.M.; error bars are not visible when smaller than then symbol). White dots, data collected in the presence of 2.3 mM isoflurane (+Iso). Data were fit through linear regression (left, $R^2 = 0.98$; right, $R^2 = 0.81$; slope > 0 for both at $P < 0.02$).

LyTASK from *L. stagnalis* is a volatile anesthetic-activated homolog of TASK-3 that shares ~47% amino acid identity (Andres-Enguix et al., 2007). Introduction of cysteine at an equivalent residue in LyTASK (i.e., L159C) conferred NEM activation on this channel (with 1 mM NEM, 121 ± 18%, $\tau = 56 \pm 7$ s; $n = 3$) (Supplemental Fig. 2); NEM had minimal effects on wild-type LyTASK (Supplemental Fig. 2).

Amino Acid Identity at Residue 159 Has Effects on Basal Currents, pH Regulation, and Isoflurane Activation. Because NEM modification effectively increases residue 159 size and alters other physicochemical attributes, we analyzed the effects of residue 159 identity on TASK-3 basal currents. Figure 4A shows that larger and/or more-hydrophobic residues at residue 159 (Trp and Phe), like NEM modification, increased basal currents, relative to smaller substitutions (Cys, Ala, and the wild-type Met residue) (Fig. 4A). To characterize further the impact of residue 159 on isoflurane regulation, we also quantified each mutant's response to isoflurane. All residue 159 mutants studied decreased isoflurane activation (Fig. 4B; Supplemental Fig. 3). Because previous studies of tandem-pore potassium channels established

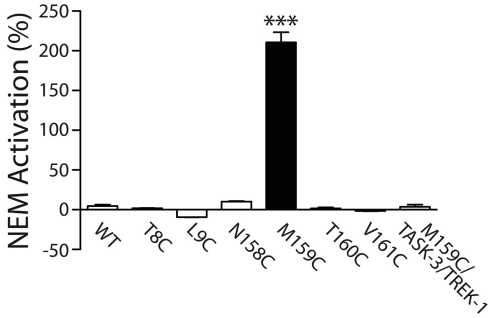

Fig. 3. NEM activation of TASK-3 potassium current is unique to Cys-159 modification and is impaired by TASK-3/TREK-1 mutation. Data were derived from current records of FRT monolayers transfected with wild-type (WT) TASK-3 or a TASK-3 mutant subunit. Current magnitude 5 min (and 3 min, in the case of M159C/TASK-3/TREK-1) after NEM (1 mM) application, relative to basal levels, was used to calculate activation, as described in *Materials and Methods*. The TASK-3/TREK-1 mutation is amino acids 243 to 248 (VLRFLT) mutated to GDWLRV. ***, significance relative to the wild-type subunit and each of the other mutants ($P < 0.001$, one-way analysis of variance and post hoc Newman-Keuls test; $n = 3–6$, mean ± S.E.M. for each).

a link between basal activity and pH regulation (Bagriantsev et al., 2011), we also studied the effect of residue 159 and NEM modification of Cys-159 on TASK-3 regulation by acidic pH. M159F and M159W mutants, relative to wild-type TASK-3, were more resistant to inhibition by acidic pH (pK_a values of 5.9, 6.0, and 6.2, respectively) (Fig. 4C). Likewise, NEM modification of Cys-159 made M159C more resistant to inhibition by acidic pH, changing its pK_a from 6.3 to 6.1 (Fig. 4C; Supplemental Fig. 4).

NEM Modification of a Single Cysteine within a TASK-3 Dimer Is Sufficient for Activation. Two TASK-3 subunits constitute a functional potassium channel, with each contributing an identical residue 159. To determine whether one or both Cys-159 residues must be modified for activation, we introduced the M159C mutation into a single subunit of a TASK-3 dimer expressed as a single peptide. The wild-type/M159C dimer channel was potentiated by NEM (Fig. 5A). We next determined whether the residue 159 identity in one subunit affects NEM modification of Cys-159 in the adjoining subunit. Larger and more-hydrophobic substitutions at residue 159, relative to the wild-type residue (i.e., M159W/M159C and M159F/M159C), but not smaller and less-hydrophobic substitutions (i.e., M159A/M159C) increased basal currents and NEM modification rates while decreasing NEM activation (Fig. 5, B and C).

m1 Muscarinic GPCR Activity Slows Cys-159 NEM Modification and Increases Apparent Activation. Because m1 muscarinic GPCR activity inhibits TASK-3, we studied its effect on Cys-159 modification. In these studies, M159C TASK-3 channels were inhibited by m1 muscarinic GPCR activation before NEM application. After inhibition, the NEM modification rate was slowed and apparent activation was markedly increased (Fig. 6, A and C). NEM caused a small but significant decrease in m1 GPCR inhibition in control studies using wild-type TASK-3 (87 ± 2 and 73 ± 2% inhibition by 100 μM carbachol in the absence and presence of 1 mM NEM at 5 min, respectively; $n = 5$; $P < 0.001$). However, coexpression of M159C TASK-3 with a constitutively active, phospholipase C-defective, $G\alpha_q$ subunit with the mutations Q209L, R256A, and T257A [$G\alpha_q$* (AA)] mirrored the effects of m1 GPCRs (Fig. 6, B and C).

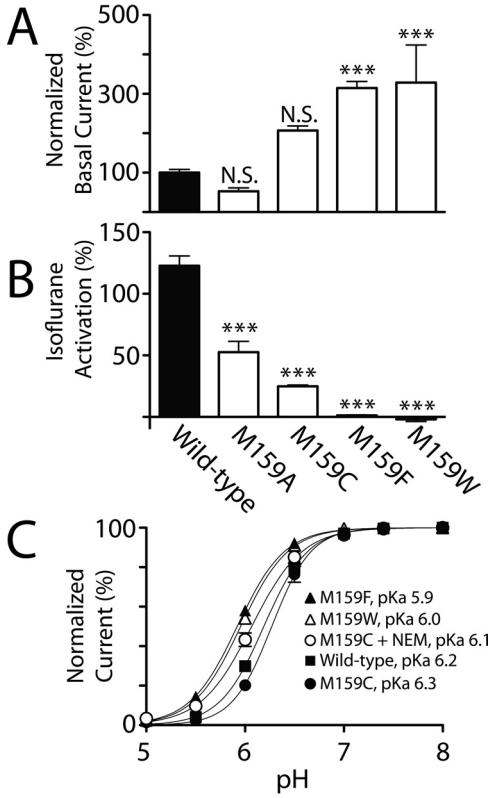

Fig. 4. Effects of residue 159 amino acid identity on TASK-3 basal currents (A), isoflurane activation (B), and pH regulation (C). Data were derived from current records of FRT monolayers transfected with wild-type TASK-3 or the indicated TASK-3 mutant (see also Supplemental Figs. 3 and 4). A and B, basal current levels and activation by isoflurane (2.3 mM). In A, the average basal current values from monolayers transfected with wild-type TASK-3 were used for normalization; monolayers used in this analysis were transfected in parallel and under identical conditions and were studied on the same day. C, effect of residue 159 or 5 mM NEM modification of Cys-159 on TASK-3 pK_a. Data, normalized to the average current at pH 8.0, were fit as follows: $I = 100/[1 + 10^{(pK_a - pH) \cdot n_H}]$, where n_H is Hill slope. pK_a values derived from each data set were significantly different from each other ($P < 0.001$), with the following values: wild-type, 6.190 (95% confidence interval, 6.173–6.206); M159C, 6.270 (95% confidence interval, 6.243–6.296); M159C plus NEM, 6.067 (95% confidence interval, 6.035–6.098); M159F, 5.920 (95% confidence interval, 5.908–5.933); M159W, 5.955 (95% confidence interval, 5.945–5.966). ***, significance relative to wild-type TASK-3 ($P < 0.001$, one-way analysis of variance and post hoc Bonferroni test; $n = 4–6$, mean ± S.E.M. for each). N.S., no significant difference relative to the wild-type TASK-3 ($P > 0.05$).

Residue 159 Modifies TASK-3 m1 GPCR Regulation. The large increase in apparent NEM activation of M159C TASK-3 with m1 GPCR or $G\alpha_q$* (AA) inhibition suggested that NEM modification was rendering M159C resistant to m1 GPCR and $G\alpha_q$* (AA) effects. To confirm this, we studied m1 GPCR regulation of M159C before and after NEM modification. At baseline, M159C regulation by m1 GPCRs was identical to that of wild-type TASK-3 (Fig. 7, A and C). As suggested, however, NEM modification rendered M159C resistant to m1 GPCR regulation (Fig. 7, B and C). Because NEM may directly antagonize m1 GPCRs and downstream signaling, we also studied the M159F and M159W TASK-3 mutants. Like NEM-modified M159C, the M159F and M159W mutants were resistant to regulation by m1 GPCRs (Fig. 7C).

m1 Muscarinic GPCR Activity Slows Isoflurane Activation and Increases Apparent Activation. To determine whether there were parallels between NEM and isoflurane

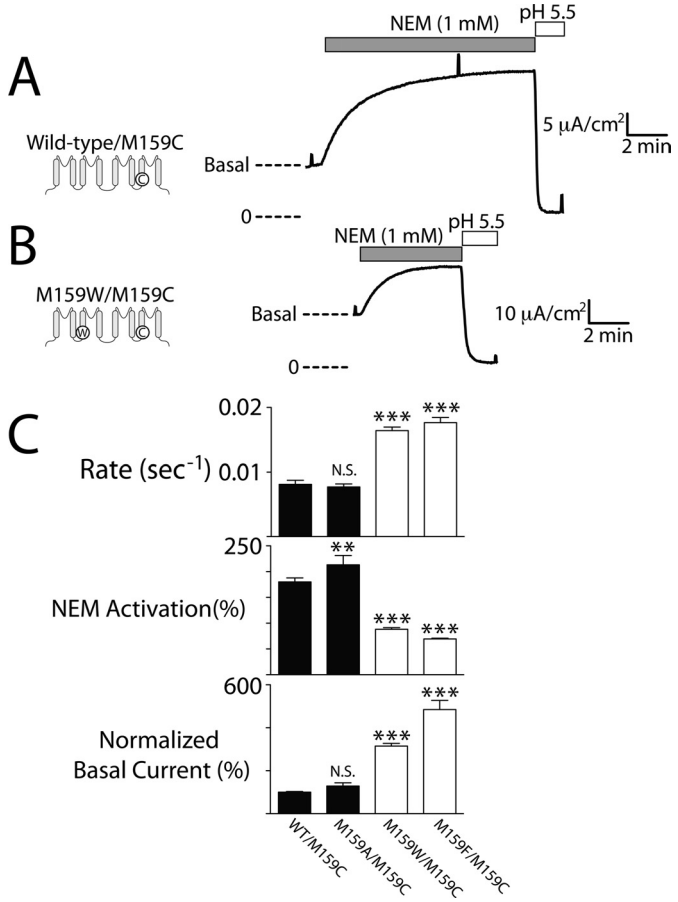

Fig. 5. Sufficiency of modification of a single Cys-159 in TASK-3 dimers for activation, revealing cross-talk between subunits. A and B, Ussing chamber transepithelial current records from FRT monolayers transfected with wild-type/M159C or M159W/M159C dimer cDNA. C, effects of residue identity at position 159 on the rate of Cys-159 modification in the adjoining subunit, NEM-mediated activation, and basal current magnitude. Data in C were derived from a single exponential fit to individual current records, as described in *Materials and Methods*. Basal currents were normalized by using average currents from monolayers transfected with wild-type/M159C dimer cDNA; monolayers used in this analysis were transfected in parallel, under identical conditions, and studied on the same day. ***, $P < 0.001$; **, $P < 0.01$, significance relative to the wild-type/M159C dimer, one-way analysis of variance and post hoc Newman-Keuls test ($n = 6$–10, mean ± S.E.M. for each). N.S., no significant difference relative to the wild-type/M159C dimer ($P > 0.05$).

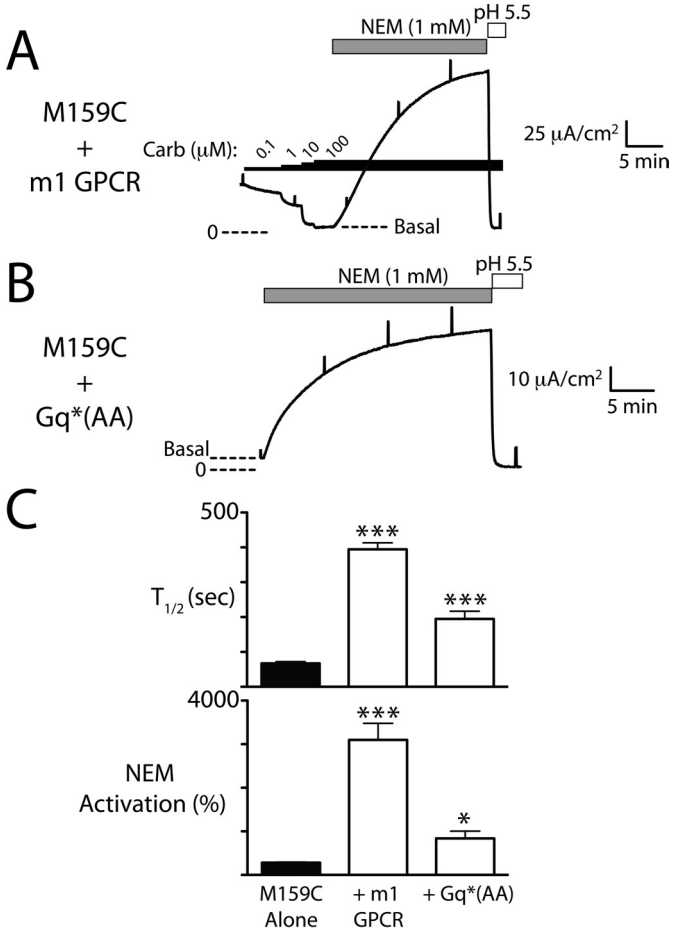

Fig. 6. m1 muscarinic GPCR and $G\alpha_q$ inhibition of TASK-3 M159C potassium current, slowing Cys-159 modification by NEM and increasing apparent NEM-mediated activation. A, current record from a FRT monolayer stably expressing m1 GPCRs and transfected with M159C TASK-3. Black bars, application of carbachol, an m1 GPCR agonist. B, current record from a FRT monolayer cotransfected with M159C TASK-3 and $G\alpha_q$* (AA). C, effect of m1 GPRC activity (using 100 μM carbachol) or $G\alpha_q$* (AA) coexpression on the magnitude of NEM-mediated activation and the rate of Cys-159 modification. Because data were not well fit by an exponential function, the time to reach half the full NEM effect ($T_{1/2}$) is reported. ***, $P < 0.001$; *, $P < 0.05$, significance relative to M159C alone, one-way analysis of variance and post hoc Newman-Keuls test [$n = 7$, 3, and 10, mean ± S.E.M., for M159C alone, plus m1 GPCRs, and plus $G\alpha_q$* (AA), respectively].

activation of TASK-3, we studied the effects of m1 GPCR activity on isoflurane activation of wild-type TASK-3 channels. As observed with NEM and M159C TASK-3, the wild-type TASK-3 isoflurane activation rate was slowed and the magnitude of apparent isoflurane activation was increased by m1 muscarinic GPCR activity (Fig. 8). Similar to the effects of NEM on M159C TASK-3 (Fig. 7B), wild-type TASK-3 channels activated by isoflurane (2.3 mM) were resistant to inhibition by m1 GPCR activity [32 ± 1% ($n = 8$) versus 66 ± 1% ($n = 9$) current remaining with 10 μM carbachol in the absence or presence of isoflurane, respectively; $P < 0.001$, Student's t test] (see also Supplemental Fig. 5).

Discussion

In this study, we determined that NEM covalent modification of Cys-159 in TASK-3 (M159C) and LyTASK (L159C) markedly increased channel activity. We found that M159C TASK-3 channels were modified by NEM more slowly and were activated to a greater extent in the presence of active m1 GPCRs or $G\alpha_q$* (AA), which paralleled isoflurane effects on wild-type TASK-3. The TASK-3/TREK-1 mutation, which renders TASK-3 resistant to anesthetic activation, rendered M159C TASK-3 resistant to NEM activation. NEM-modified M159C TASK-3, like isoflurane-activated wild-type TASK-3, was resistant to inhibition by m1 GPCR activity. Channels with larger or more-hydrophobic side chains (M159W and M159F TASK-3) had increased channel activity and were resistant to inhibition by m1 GPCR activity. NEM modification of Cys-159 made channels more resistant to inhibition by acidic pH, as did mutagenesis of residue 159 to Trp or Phe. Finally, TASK-3 dimer studies determined that modification of a single Cys-159 was sufficient for channel activation. The dimer studies also provided evidence of cross-talk between TASK-3 subunits, inasmuch as the residue 159 identity in

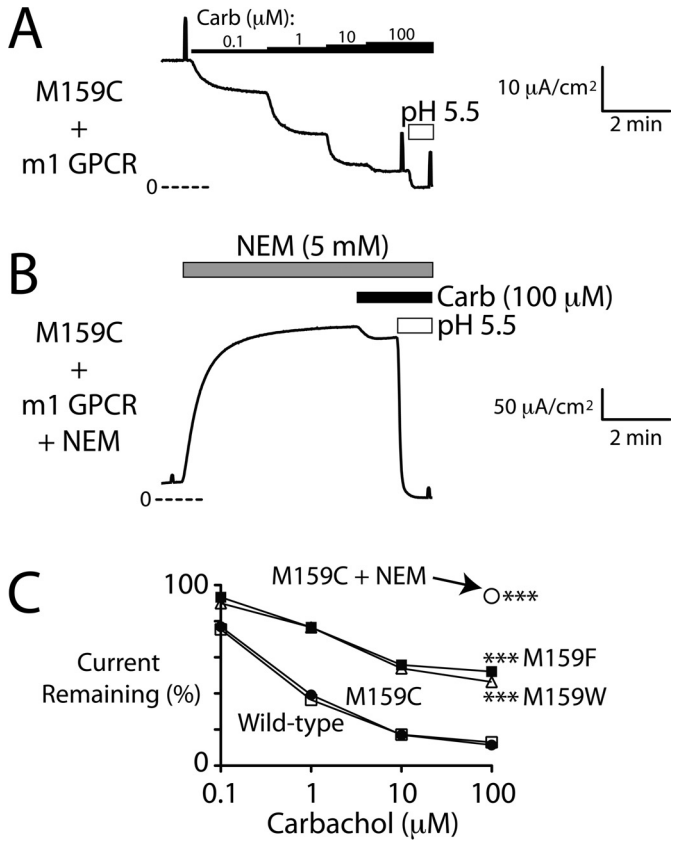

Fig. 7. Residue 159 modification of m1 muscarinic GPCR inhibition. A and B, current records from FRT monolayers stably expressing m1 GPCRs and transfected with M159C TASK-3. Carbachol (Carb), an m1 GPCR agonist, was added in the absence (A) or presence (B) of NEM modification. C, carbachol concentration-dependent responses of FRT monolayers transfected with wild-type, M159C (with or without 5 mM NEM), M159F, or M159W TASK-3 cDNA. In C, each monolayer's response is normalized to its own steady-state, basal current just before carbachol application. Comparison was made at the 100 μM carbachol concentration only. ***, significance relative to both wild-type and M159C TASK-3, $P < 0.001$, one-way analysis of variance and post hoc Newman-Keuls test (n = 3–6, mean ± S.E.M.; error bars are not shown when smaller than the symbol). There was no significant difference between M159C and wild-type TASK-3 ($P > 0.05$).

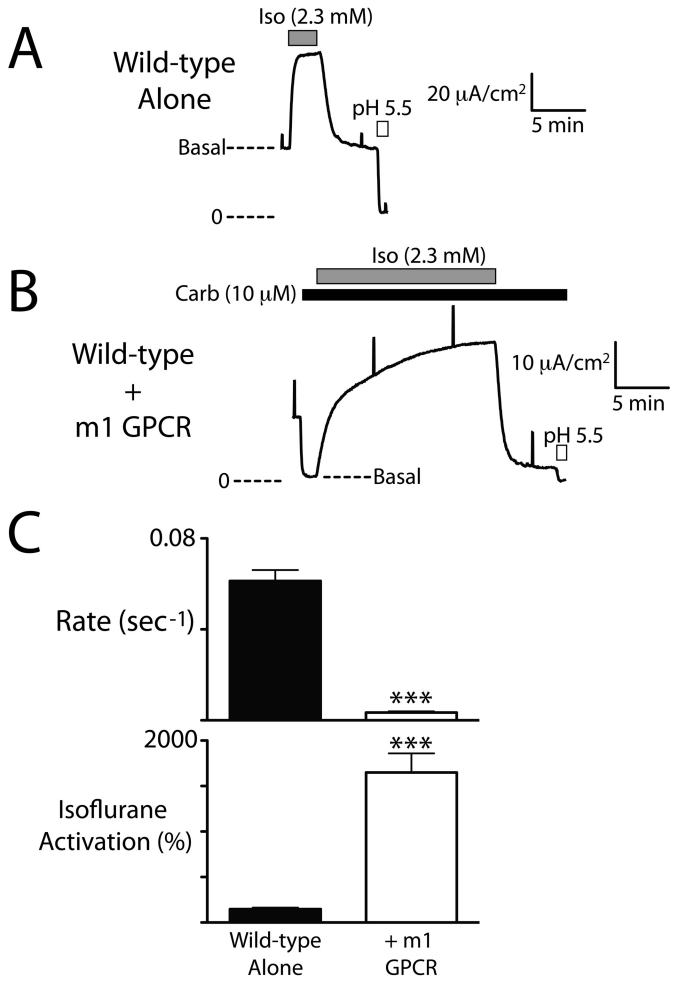

Fig. 8. m1 muscarinic GPCR inhibition of wild-type TASK-3 potassium current, slowing isoflurane (Iso) activation and increasing isoflurane-mediated activation. A, current record from a FRT monolayer transfected with wild-type TASK-3. B, current record from a FRT monolayer stably expressing m1 muscarinic GPCRs and transfected with wild-type TASK-3. Black bar, application of carbachol (Carb), a m1 GPCR agonist. C, effect of m1 GPCR activation (10 μM carbachol) on the rate and magnitude of isoflurane activation. Data from wild-type TASK-3 alone were fit with a one-phase exponential function. After inhibition by m1 GPCRs, isoflurane effects on the TASK-3 potassium current signal were best fit by a two-phase exponential function; a composite rate constant (see *Materials and Methods*) was derived to facilitate comparison with data collected in the absence of m1 GPCR effects. ***, significance relative to wild-type TASK-3 alone, $P < 0.001$, unpaired Student's t test (n = 8, mean ± S.E.M.).

one subunit altered the Cys-159 modification rate of the other subunit.

Contribution of Residue 159 to Volatile Anesthetic Binding. Volatile anesthetics have been shown to interact with proteins in a manner consistent with the Meyer-Overton hypothesis (Franks and Lieb, 1984), and identifying the anesthetic binding site on a protein or ion channel is an important step in understanding anesthetic regulation. Andres-Enguix et al. (2007) identified residue 159 as being critical for volatile anesthetic activation of TASK channels. Because the L159A mutation eliminated LyTASK isoflurane stereoselectivity in its residual isoflurane activation, residue 159 may have a role in anesthetic binding. However, the possibility of indirect or allosteric effects beyond direct binding is difficult to exclude. We determined that M159C TASK-3, like M159A, was minimally affected by isoflurane (Fig. 4). Because M159C is activated by NEM, the M159C mutation likely does not eliminate isoflurane activation by "locking" the channel in an open state. This presupposes, of course, that NEM acts primarily on channel gating and not on conductance or acute surface expression.

If NEM and isoflurane compete for a common interaction site on TASK-3, then NEM modification of TASK-3 should be slowed by isoflurane; however, that is not what we found (Fig. 2C). There are three potential explanations for this result. First, M159C demonstrates diminished activation by isoflurane, such that isoflurane may only minimally interact with M159C TASK-3. Second, we found that activating amino acid substitutions (i.e., M159W and M159F) increased the rate of NEM modification of the adjoining Cys-159. Therefore, by inference, isoflurane binding near one Cys-159 may enhance NEM modification of the other Cys-159. Third, Cys-159 may not reside in an isoflurane binding site and effects on isoflurane regulation of TASK-3 may be indirect and/or allosteric.

Relative to Met-159 in the wild-type channel, both smaller

residues (Cys-159 and Ala-159) and larger residues (Trp-159 and Phe-159) decreased isoflurane activation (Fig. 4). It may be that smaller residues fail to provide sufficient interaction with the anesthetic, whereas larger residues may mimic the drug while simultaneously excluding it. Consistent with this, M159F and M159W mutations seemed to activate TASK-3, with increased basal currents. We acknowledge that increased surface expression, and not gating, might explain the increased basal currents. Our results are consistent with Met-159 having a role in anesthetic binding, but they certainly are not conclusive.

Contribution of Residue 159 to Regulation by m1 Muscarinic GPCRs and Active $G\alpha_{q/11}$. $G\alpha_{q/11}$-coupled GPCRs promote central nervous system arousal in part through inhibition of TASK-3 and other potassium channels (Franks, 2008). Several such GPCRs (e.g., m1/3 muscarinic, OX1/2 orexin, H1 histamine, and α1-adrenergic receptors) are targeted by the ascending arousal pathways of the brain that are essential for maintenance of consciousness and/or recovery from general anesthesia (Steriade et al., 1993; Hudetz et al., 2003; Kelz et al., 2008; Luo and Leung, 2009). The molecular mechanism by which $G\alpha_{q/11}$-coupled GPCRs regulate TASK-3 is unclear. Chen et al. (2006) demonstrated direct binding of activated $G\alpha_{q/11}$ to TASK-3 as one mechanism by which GPCRs inhibit TASK-3; however, others have suggested that PIP_2 depletion may (Czirják et al., 2001; Chemin et al., 2003; Kang et al., 2006) or may not (Chen et al., 2006; Lindner et al., 2011) have a role. We determined that NEM modified Cys-159 more slowly in the presence of activated m1 GPCRs and $G\alpha_q$* (AA). The decreased modification rate with m1 GPCRs and $G\alpha_q$* (AA) suggests that Cys-159 modification is at least partially rate-determining for M159C activation and that activation is not limited by other factors, such as passage through the membrane. We speculate that activated $G\alpha_{q/11}$ and/or other factors related to m1 GPCR signaling (e.g., depleted PIP_2 levels) may sequester M159C channels in a state in which Cys-159 is less reactive with NEM, for steric or other reasons. We also determined that NEM-modified M159C was resistant to m1 GPCR inhibition. Some of this effect may be attributable to NEM inhibition of m1 GPCR signaling or modification of the $G\alpha_q$* (AA) protein. In control studies, however, NEM effects on m1 GPCR activity were minimal, and M159F and M159W were also resistant to m1 GPCR inhibition (Fig. 7). NEM modification, or the M159F and M159W mutations, may directly impair active $G\alpha_{q/11}$ binding with TASK-3 or may indirectly stabilize a state in which active $G\alpha_{q/11}$ binding is less favored.

TASK-3 Dimer Studies. TASK-3 channels are composed of two subunits (i.e., a dimer), with each contributing an identical residue 159. The M159C NEM modification rate was linear with respect to NEM concentrations, which suggests that modification of a single Cys-159 was sufficient for TASK-3 activation (Fig. 2C). In agreement, TASK-3 dimers containing a single M159C were activated by NEM (Fig. 5). This observation suggests that residue 159 in one subunit can have a "dominant" effect over the other subunit in TASK-3 function. It is noteworthy that M159W and M159F mutations, which activate TASK-3 function, decreased NEM activation magnitude within dimers, which implies that Trp-159 and Phe-159 were dominant over the adjoining Cys-159 in promoting an open state. It is noteworthy that Trp-159 and Phe-159 increased the rate of NEM modification of the adjoining Cys-159. This provides evidence of cross-talk between the residues 159. It may be that both residues 159 contribute to a single common site on the channel that is accessed by NEM; however, it seems more likely they interact through a conformational change, because Cys-159 modification is expedited and not slowed by the bulky Trp-159 and Phe-159 residues.

Relevance of NEM to Volatile Anesthetic Regulation. The purpose of our study was to better understand volatile anesthetic regulation of TASK-3 channels. NEM is not a general anesthetic and, on the basis of its hydrophobicity (i.e., its calculated log*P*), would have an anesthetic potency greater than 100 mM. Several observations, however, suggest that NEM is interacting with TASK-3 in a manner relevant to isoflurane. 1) The TASK-3/TREK-1 mutation eliminates both NEM and isoflurane activation (Fig. 3). 2) NEM activates TASK-3 via a mutation (M159C) that simultaneously disrupts isoflurane activation (Fig. 4). 3) m1 GPCR inhibition of TASK-3 similarly affects both NEM and isoflurane activation (both slowing the rate and increasing the apparent magnitude of activation) (Figs. 6 and 8). 4) NEM-modified M159C TASK-3 and isoflurane-activated wild-type TASK-3 are both resistant to m1 GPCR inhibition. This last observation conflicts with previous studies that demonstrated similar GPCR-mediated inhibition of TASK-3 or TASK-like currents in the presence or absence of halothane (Sirois et al., 2002; Talley and Bayliss, 2002). The discrep-

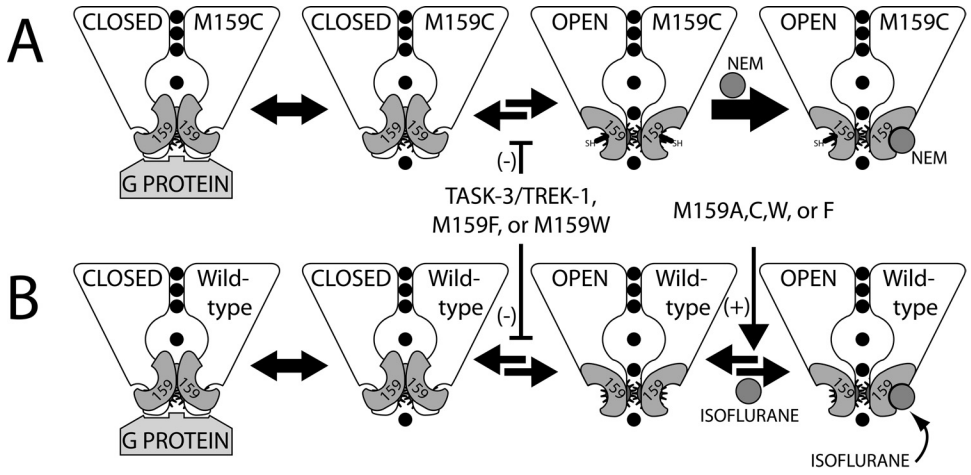

Fig. 9. Model illustrating effect of Cys-159 NEM modification in M159C (A) and isoflurane binding in wild-type TASK-3 (B). Irreversible NEM modification of a single thiol provided by either of the two Cys-159 residues stabilizes M159C TASK-3 in an open state. Likewise, isoflurane binding at one of two analogous sites in wild-type TASK-3 stabilizes an open state (not shown). PIP_2 interacts with the open state. The residues at position 159 are coupled via gears to illustrate the observed cross-talk between them. Transition into a closed state causes decreased accessibility of NEM to the Cys-159 thiol and of isoflurane to its binding site. Transition into a closed state is required for interaction with activated $G\alpha_q$ protein and is impeded by M159W, M159F, and the TASK-3/TREK-1 mutations. Mutations at Met-159 decrease isoflurane binding by enhancing its off-rate.

ancy might be attributable to differences in the choice of agonist concentration, anesthetic type and/or concentration, GPCR type and/or relative expression, and/or cell type. Guided by concentration-response data, we selected a submaximal carbachol concentration for optimal detection of isoflurane-induced changes in agonist potency.

Summary Model. Our findings for this study are summarized in Fig. 9. In this model, the Cys-159 of M159C TASK-3 is more accessible in the open state and is "protected" in the closed state (Fig. 9A). A parallel scheme for isoflurane interaction with wild-type TASK-3 is also shown (Fig. 9B). PIP_2 interacts with open TASK-3. Active $G\alpha_{q/11}$ interacts with closed TASK-3, and interventions that stabilize TASK-3 in an open state minimize this interaction. We speculate that TASK-3/TREK-1 and M159F or M159W mutations inhibit transition to a closed state. The effects of this are two-fold; 1) it impairs regulation of these mutants by active $G\alpha_{q/11}$, and 2) it decreases NEM and isoflurane apparent activation. The two NEM modification or isoflurane binding sites are coupled. We also hypothesize that Met-159 mutations decrease the binding affinity of isoflurane and thereby increase its off-rate.

In conclusion, our data suggest that volatile anesthetics bind at a single site near Met-159 and "prop" TASK-3 in an open state that is resistant to regulation by arousal-promoting GPCRs. The tools developed in this study should be useful for investigating this hypothesis and scrutinizing the interactions between active $G\alpha_{q/11}$, volatile anesthetics, and TASK-3.

Acknowledgments

We thank Drs. Stuart Forman, Thomas Gardella, Keith Miller, Douglas Raines, Ken Solt, and C. Spencer Yost for helpful discussions and review of the manuscript. Thanks also go to Phil Karp, Dr. Pete Snyder, and Dr. Michael Welsh (University of Iowa) for assistance with the FRT cell line.

Authorship Contributions

Participated in research design: Conway and Cotten.

Conducted experiments: Cotten.

Contributed new reagents or analytic tools: Conway and Cotten.

Performed data analysis: Cotten.

Wrote or contributed to the writing of the manuscript: Conway and Cotten.

References

Andres-Enguix I, Caley A, Yustos R, Schumacher MA, Spanu PD, Dickinson R, Maze M, and Franks NP (2007) Determinants of the anesthetic sensitivity of two-pore domain acid-sensitive potassium channels: molecular cloning of an anesthetic-activated potassium channel from *Lymnaea stagnalis*. *J Biol Chem* **282:**20977–20990.

Bagriantsev SN, Peyronnet R, Clark KA, Honoré E, and Minor DL Jr (2011) Multiple modalities converge on a common gate to control K2P channel function. *EMBO J* **30:**3594–3606.

Chemin J, Girard C, Duprat F, Lesage F, Romey G, and Lazdunski M (2003) Mechanisms underlying excitatory effects of group I metabotropic glutamate receptors via inhibition of 2P domain K^+ channels. *EMBO J* **22:**5403–5411.

Chen X, Talley EM, Patel N, Gomis A, McIntire WE, Dong B, Viana F, Garrison JC, and Bayliss DA (2006) Inhibition of a background potassium channel by Gq protein alpha-subunits. *Proc Natl Acad Sci USA* **103:**3422–3427.

Cotten JF and Welsh MJ (1998) Covalent modification of the nucleotide binding domains of cystic fibrosis transmembrane conductance regulator. *J Biol Chem* **273:**31873–31879.

Czirják G, Petheo GL, Spät A, and Enyedi P (2001) Inhibition of TASK-1 potassium channel by phospholipase C. *Am J Physiol Cell Physiol* **281:**C700–C708.

Franks NP (2008) General anaesthesia: from molecular targets to neuronal pathways of sleep and arousal. *Nat Rev Neurosci* **9:**370–386.

Franks NP and Lieb WR (1984) Do general anaesthetics act by competitive binding to specific receptors? *Nature* **310:**599–601.

Franks NP and Lieb WR (1993) Selective actions of volatile general anaesthetics at molecular and cellular levels. *Br J Anaesth* **71:**65–76.

Hudetz AG, Wood JD, and Kampine JP (2003) Cholinergic reversal of isoflurane anesthesia in rats as measured by cross-approximate entropy of the electroencephalogram. *Anesthesiology* **99:**1125–1131.

Kang D, Han J, and Kim D (2006) Mechanism of inhibition of TREK-2 (K2P10.1) by the Gq-coupled M3 muscarinic receptor. *Am J Physiol Cell Physiol* **291:**C649–C656.

Kelz MB, Sun Y, Chen J, Cheng Meng Q, Moore JT, Veasey SC, Dixon S, Thornton M, Funato H, and Yanagisawa M (2008) An essential role for orexins in emergence from general anesthesia. *Proc Natl Acad Sci USA* **105:**1309–1314.

Kim Y, Bang H, and Kim D (2000) TASK-3, a new member of the tandem pore K^+ channel family. *J Biol Chem* **275:**9340–9347.

Lazarenko RM, Willcox SC, Shu S, Berg AP, Jevtovic-Todorovic V, Talley EM, Chen X, and Bayliss DA (2010) Motoneuronal TASK channels contribute to immobilizing effects of inhalational general anesthetics. *J Neurosci* **30:**7691–7704.

Lindner M, Leitner MG, Halaszovich CR, Hammond GR, and Oliver D (2011) Probing the regulation of TASK potassium channels by $PI(4,5)P_2$ with switchable phosphoinositide phosphatases. *J Physiol* **589**:3149–3162.

Lobo IA, Trudell JR, and Harris RA (2006) Accessibility to residues in transmembrane segment four of the glycine receptor. *Neuropharmacology* **50:**174–181.

Luo T and Leung LS (2009) Basal forebrain histaminergic transmission modulates electroencephalographic activity and emergence from isoflurane anesthesia. *Anesthesiology* **111:**725–733.

Pang DS, Robledo CJ, Carr DR, Gent TC, Vyssotski AL, Caley A, Zecharia AY, Wisden W, Brickley SG, and Franks NP (2009) An unexpected role for TASK-3 potassium channels in network oscillations with implications for sleep mechanisms and anesthetic action. *Proc Natl Acad Sci USA* **106:**17546–17551.

Patel AJ, Honoré E, Lesage F, Fink M, Romey G, and Lazdunski M (1999) Inhalational anesthetics activate two-pore-domain background K^+ channels. *Nat Neurosci* **2:**422–426.

Sheppard DN, Carson MR, Ostedgaard LS, Denning GM, and Welsh MJ (1994) Expression of cystic fibrosis transmembrane conductance regulator in a model epithelium. *Am J Physiol* **266:**L405–L413.

Sirois JE, Lynch C 3rd, and Bayliss DA (2002) Convergent and reciprocal modulation of a leak K^+ current and I_h by an inhalational anaesthetic and neurotransmitters in rat brainstem motoneurones. *J Physiol* **541:**717–729.

Steriade M, McCormick DA, and Sejnowski TJ (1993) Thalamocortical oscillations in the sleeping and aroused brain. *Science* **262:**679–685.

Talley EM and Bayliss DA (2002) Modulation of TASK-1 (Kcnk3) and TASK-3 (Kcnk9) potassium channels: volatile anesthetics and neurotransmitters share a molecular site of action. *J Biol Chem* **277:**17733–17742.

Yost CS (2003) Update on tandem pore (2P) domain K^+ channels. *Curr Drug Targets* **4:**347–351.

Address correspondence to: Dr. Joseph F. Cotten, Massachusetts General Hospital, Department of Anesthesia, Critical Care, and Pain Medicine, 55 Fruit St, GRB 444, Boston, MA 02114. E-mail: jcotten@partners.org